Transonic Wind-Tunnel and Flight Buffet Pressures on a Swept Wing

C. E. Lemley* and R. E. Mullans†
McDonnell Aircraft Company, St. Louis, Mo.

Wind-tunnel tests to measure buffeting flow characteristics and dynamic wing response on a 10% scale model of the F-4 airplane have provided an empirical basis for the prediction of transonic buffet pressure distribution on high performance fighter wings. Angle-of-attack and Mach number were primary variables in the test that incorporated wide-band pressure transducers, accelerometers, and strain gages. Sensor arrangement indicated the nature of pressures at discrete points and also the correlation between pressures at different locations. Data were compared with full scale flight measurements, and results include root mean square pressure distributions as well as spectral characteristics.

Introduction

THE type of airplane wing buffet investigated here occurs when an aircraft is in a high angle-of-attack flight regime and the air flow on the upper wing surface becomes detached. Air flow in the detached regions becomes turbulent thereby giving rise to fluctuating pressures on the wing and the possibility of induced pressures on the tail. While some loss of lift may be experienced, there is an appreciable range of angles-of-attack beyond the buffet boundary in which an airplane can maneuver. The upper limit is usually determined by wing rock or stall.

Buffet investigations that have dealt with aircraft can be divided into two distinct time periods—those that occurred prior to the intensive U.S. space effort which dominated the late 1950's and 1960's, and those which have occurred since about 1968. Impetus for the earlier studies was provided mainly by the necessity to understand the nature and severity of the buffeting loads and their potentially destructive effect on aircraft structures. The more recent studies have, in a sense, been a continuation of the earlier efforts. However, the scope of needed buffet investigations has been greatly increased by the desire to utilize aircraft maneuver capabilities beyond buffet onset even well into the transonic flight regime. The Air Force[1-3] and NASA[4-6] have conducted in-depth investigations of buffet both analytically and experimentally and Ref. 7 indicates some of the effort being carried on in Great Britain. Most of these studies, however, have been concerned mainly with definition of buffet onset and with the measurement of mean steady pressures and loads. The use of wide band fluctuating pressure sensors to measure aircraft buffet pressures has been somewhat limited, but effort in this direction has been sponsored by the Air Force and by NASA.

Although some of the technology gained from space launch vehicle buffet studies[7,8] has been applied to aircraft, it has been found that the fluctuating buffet pressures on a highly swept airplane wing present very different characteristics. In general, the flow pattern on the upper surface of a wing deep in buffet does not exhibit a recognizable flow pattern, and it is not at all safe to assume that convected flow occurs in the streamwise direction.

This paper describes the fluctuating pressure behavior measured during wind-tunnel tests of a highly swept wing in transonic buffet. The data were used in a study program[10] to develop a method for predicting buffet dynamic loads during transonic maneuvers. The wing fluctuating pressure characteristics discussed here include: spatial variations of pressure coefficients, spectral features of pressures, and variation of fluctuating pressure coefficients with angle-of-attack and Mach number. Also described are the comparisons of wind tunnel data with flight data. The flight measurements were obtained from a previous program that is reported in Ref. 1.

Test Program

The test program consisted of two series of wind tunnel tests that were conducted on a 10% scale F-4E airplane model in the 16T tunnel at Arnold Engineering Development Center. The purpose of the first test series was to obtain flow visualization data on the upper surface of the wings and to aid in locating fluctuating pressure transducers. The purpose of the second test series was to obtain actual measurements of the time histories of pressures, accelerations, strains, and forces obtained during tunnel runs.

The model configuration was determined by the YF-4E version of the basic F-4E airplane that was used in the Ref. 1 flight test program. The full span 10% model is shown in three-view in Fig. 1. Although the model wing was equipped with leading and trailing edge flaps, the data presented here are for a clean wing, i.e., undeflected flaps. The left-hand wing was fitted with a row of oil extrusion holes 0.5 in. apart located along a line that went from about 15% chord at the wing root to about 30% chord at the wing tip. These holes were fed from a common manifold imbedded in the wing.

The flow visualization phase of wind-tunnel testing consisted of obtaining still and moving pictures of oil flow and tuft patterns. The left-hand wing was equipped with the oil orifices and had its upper surface painted white to provide contrast with colored oil. The upper surface of the right-hand wing was painted black to provide contrast with the white nylon tufts that were attached in a rectangular grid pattern in rows approximately 1 in. apart.

Flow data were obtained in a Mach range of 0.7 to 1.2 at wing angles-of-attack between $-4°$ and $20°$. Reynolds numbers of 1.25×10^6, 2.5×10^6, and 3.75×10^6/foot were

Presented as Paper 73-311 at the AIAA Dynamics Specialists Conference, Williamsburg, Virginia, March 19–20, 1973; submitted May 7, 1973; revision received January 11, 1974. This work was conducted under U.S. Air Force Contract AF33615-70-C-1272. The authors wish to acknowledge the contributions and assistance of J. C. Houbolt who served as consultant to McDonnell Aircraft Co. on this program and to V. J. Johnson who represented the Air Force as Technical Monitor.

Index categories: Aircraft Testing (Including Component Wind Tunnel Testing); Boundary Layers and Convective Heat Transfer —Turbulent; Subsonic and Transonic Flow.

*Project Structural Dynamics Engineer.

†Senior Engineer, Structural Dynamics.

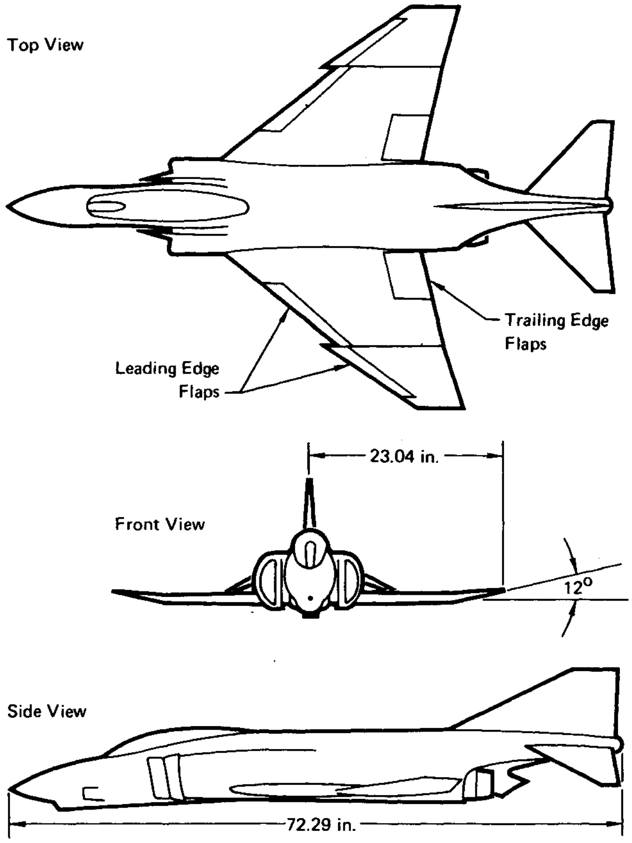

Fig. 1 General arrangement of F-4E 10% model.

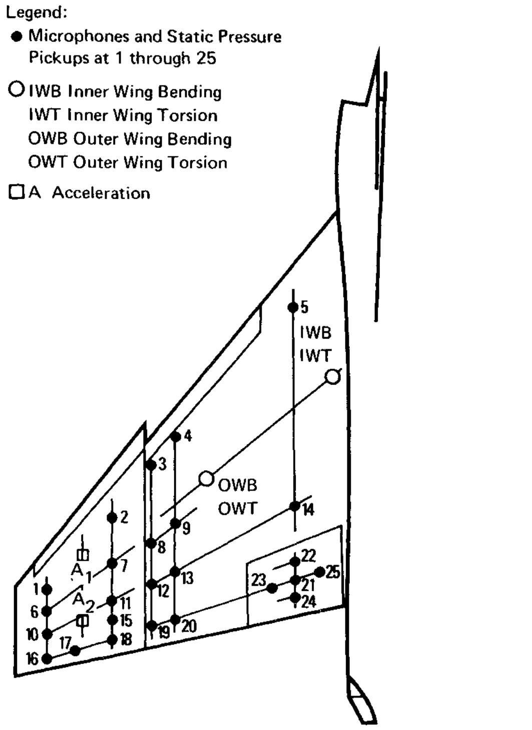

Fig. 3 Model wing instrumentation.

used. A photograph of the tuft and oil flow patterns is shown in Fig. 2.

Prior to model vibration tests, instrumentation consisting of fluctuating pressure transducers, accelerometers and strain gages was installed on the model. The pressure transducers were installed on the upper surface of the wing and tail to measure fluctuating surface pressures. Strain gages were installed at two locations on the wing and one location on the horizontal tail to measure bending and torsional strains induced during buffet. In addition to an accelerometer located at the model c.g., a pair of high frequency accelerometers was located near the wing tip to measure bending and torsion acceleration response to buffet pressure. Figure 3 shows the detailed location of the sensors on the wing. All wing mounted transducers were recessed in the wing to preserve a smooth wing contour. Leads were routed through grooves in the wing, into the fuselage and hence into the sting.

A second vibration test was made with the model installed in the wind tunnel to determine the vibration modes and frequencies that might influence buffet data measured on the model.

The buffet data acquisition tests were conducted at Mach numbers between 0.7 and 1.10. Most of the data were obtained at a Reynolds number of 3.75×10^6/foot. The wing angle-of-attack range was from $-1.5°$ to $+16°$ with 0° yaw.

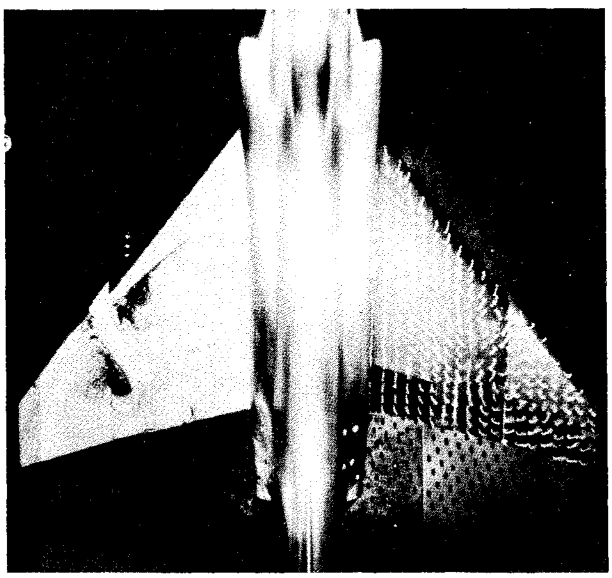

Fig. 2 Tufts and oil flow on 10% model.

Locating Pressure Transducers

The locations of the 25 wing mounted fluctuating pressure transducers (microphones) were selected by the following criteria: 1) Densely grouped in areas of high turbulence and sparsely grouped in regions of low turbulence, 2) Arranged so that flow characteristics could be readily determined, and 3) Located to provide direct comparison with flight test data. The forwardmost microphone locations shown in Fig. 3 on the inner wing panel were restricted to

Table 1 Functional grouping of fluctuating pressure transducers

Group	Transducers (see Fig. 3)	Purpose
1	1, 2, 4, 5, 6, 7, 9, 10, 11, 13, 14, 16, 18, 20, 21	Coarse grid for defining major flow features on wing
2	11, 15, 16, 17, 18	Fine grid for defining bow features on outer wing
3	2, 3, 4, 7, 8, 9, 11, 12, 13, 18, 19, 20	Investigate localized effect of snag
4	17, 18, 21, 24	Compare with flight test data

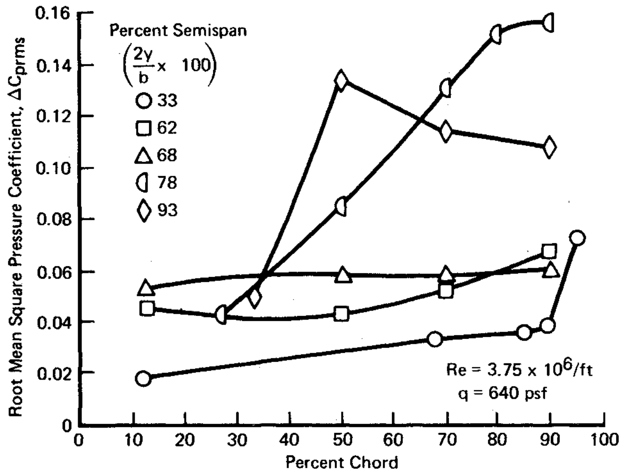

Fig. 4 Root mean square pressure coefficient vs percent chord (configuration 1, Mach 0.9, wing angle-of-attack 12°).

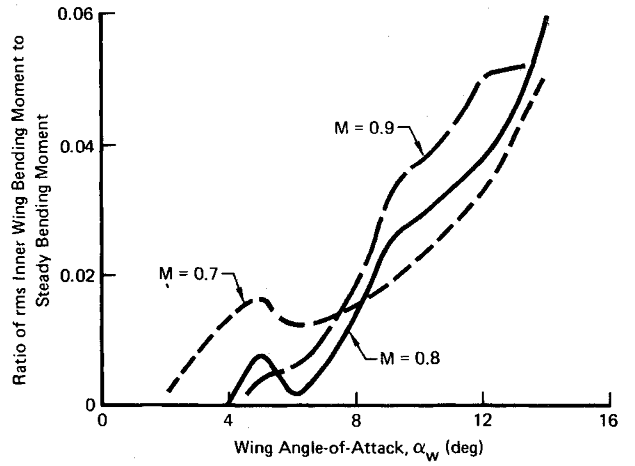

Fig. 6 Ratio of rms inner wing bending moment to steady bending moment.

the 12% chord line because of interference with the flap, and those on the outer wing panel could not be forward of the 30% chord line because of thinness of the wing and interference with the oil flow manifold. Also, transducers in the outboard panel could be located no further aft than the 90% chord because of wing thinness. Transducers 17 and 18 at 90% chord do coincide with those of flight test pickups. Functional groupings of microphones are shown in Table 1.

Twenty-four of the twenty-eight microphones used on the model were installed in mounting discs that recessed the diaphragms and protected them from possible stream carried particle impingment. Comparative frequency calibrations showed that frequency response was not affected by the mounting discs. No microphones were lost because of diaphragm damage during the buffet pressure measurement.

Test Results

Buffet onset occurred at wing angles-of-attack between 6° and 8° but was difficult to define precisely inasmuch as different indicators tend to indicate different onset angles. Most of the data, however, were obtained at wing angles-of-attack of 12° and 14° where the wing was in well developed buffet. The buffet characteristics of major interest were: spatial variation of pressure coefficients, spectral nature of fluctuating pressure, Mach number effect, and angle-of-attack effect. The spatial variation of the fluctuating pressure coefficient ΔC_{prms}, defined by

$$\Delta C_{prms} = p/q \tag{1}$$

where p is the over-all root mean square value of local fluctuating pressure and q is the freestream dynamic pressure, is shown in Fig. 4. The variation of ΔC_{prms} with spanwise and chordwise position shown in this plot is typical of the results found. The pressures were generally higher outboard, and increased from leading edge to trailing edge. The more dramatic chordwise changes were evident at the outboard locations of 78% and 93% semispan. The spectral character of the pressures is shown in Fig. 5 which is a plot showing the spectral characteristics at six locations on the wing. Model-sting natural frequencies occurring in the 15–18 Hz range appeared not to affect pressure data. The plots for locations 2, 16, and 18 show a peak at 650 Hz. Based on flow visualization studies and analysis of the static pressures over the wing, a cone-shaped region emanating from the snag is thought to contain a vortex originating at the snag. Thus the 650 Hz peaks are also thought to be caused by this vortex. The frequencies associated with the different vortices would then be related to some kind of circulation or rotation frequency of the vortices. The frequency associated with the snag vortex was generally about half that from the leading edge and tip vortices. These frequencies, scaled to the flight vehicle, were at the higher end of the vehicle primary structural resonant frequencies. The peak frequencies decreased as Mach number and angle-of-attack increased.

Diminishing power spectral densities (PSD's) between 10 and 200 Hz occur for the transducers along the tip and leading edge. Because of the locations of these transducers, it seems that they are also related to the leading edge and tip vortices although in a different manner from the spectral peaks.

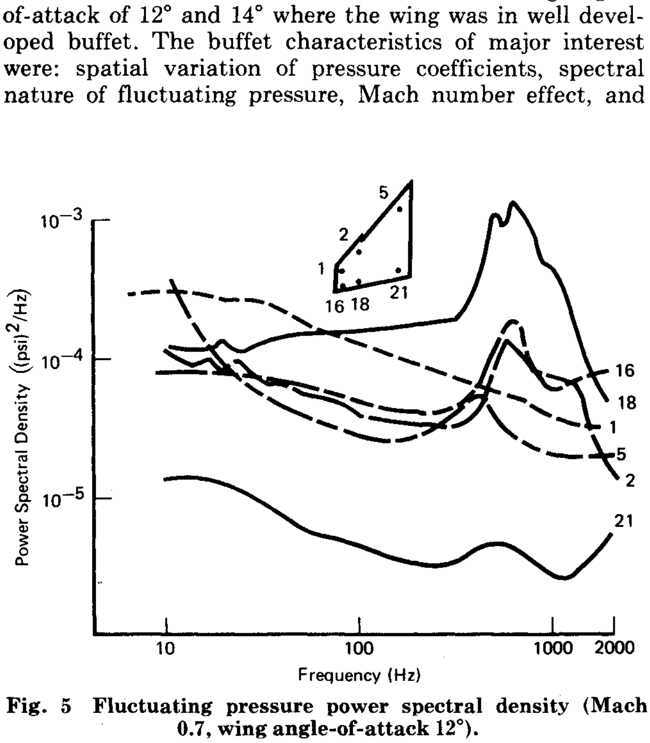

Fig. 5 Fluctuating pressure power spectral density (Mach 0.7, wing angle-of-attack 12°).

Buffet Response with Mach Number

The effect of Mach number on buffet response is demonstrated in Fig. 6 which is a plot of the wing bending strain gage output (presented as rms bending moment divided by static bending moment) vs angle-of-attack at M = 0.7, 0.8, 0.9. These curves show that the response is similar for angles between 8° and 14°. The M = 0.9 response tends to be higher at the higher angles-of-attack. Buffet response severity dropped rather abruptly at M = 1 and thereafter, so that the more severe transonic buffet response occurs below M = 1.

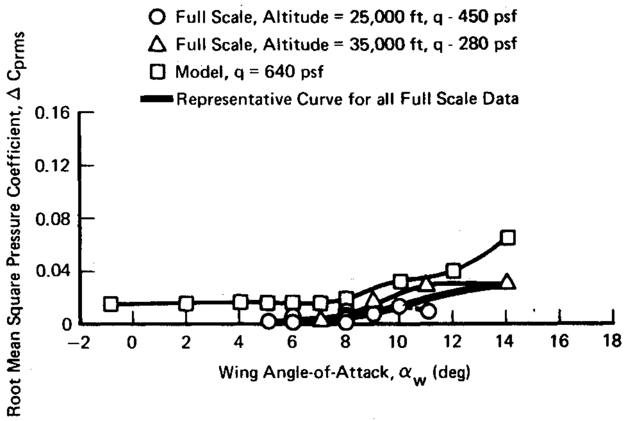

Fig. 7 Comparison of model and full scale rms pressure coefficient variation with angle-of-attack of Mach 0.9, 90% chord, 33% semispan.

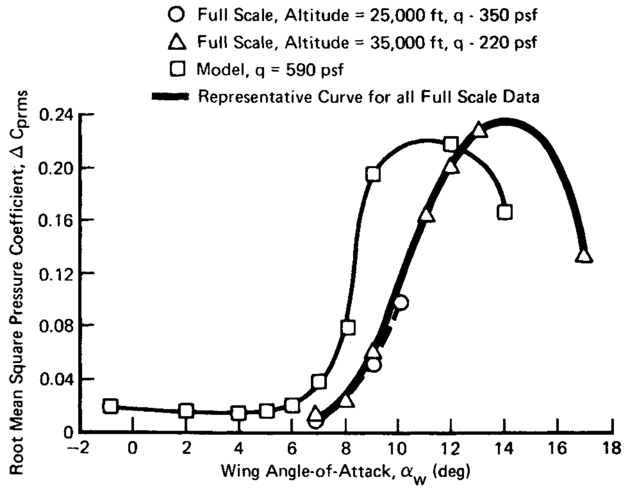

Fig. 9 Comparison of model and full scale rms pressure coefficient variation with angle-of-attack at Mach 0.8, 90% chord, 78% semispan.

Comparison of Model and Full Scale Data

Model and full scale measurements were compared at four pressure transducer locations. Comparisons made on the basis of ΔC_{prms} are shown in Figs. 7 and 8 for M = 0.9 at one inboard location and one outboard location. These plots show the trend generally observed in these tests that model measurements are larger. An additional comparison of interest is shown in Fig. 9 which clearly indicates a data shift of about 3°. It is believed that this is a result of slightly different locations of vortices originating at the leading edge snag discontinuity which may affect different areas on the model and on the full scale wing.

The plot of Fig. 10 compares spectral characteristics of fluctuating pressures measured on the wing of the model with corresponding measurements on the full scale wing. The full scale data have been scaled to model size by the following relationships:

$$f_m = (L_{fs}/L_m)(V_m/V_{fs})f_{fs} \tag{2}$$

$$G_m(f_m) = \frac{p_m^2}{p_{fs}^2}\frac{L_m}{L_{fs}}\frac{V_{fs}}{V_m}G_{fs}(f_{fs}) \tag{3}$$

where f = frequency, L = structural reference length, V = freestream velocity, G = power spectral density, psi²/Hz, p = over-all rms fluctuating pressure and the subscripts denote m = model, fs = full scale. This comparison, for M = 0.85 and wing angle-of-attack of 10°, shows that excellent agreement can be obtained and that model pressure spectral measurements can be reliably scaled to aircraft by careful control of scale parameters.

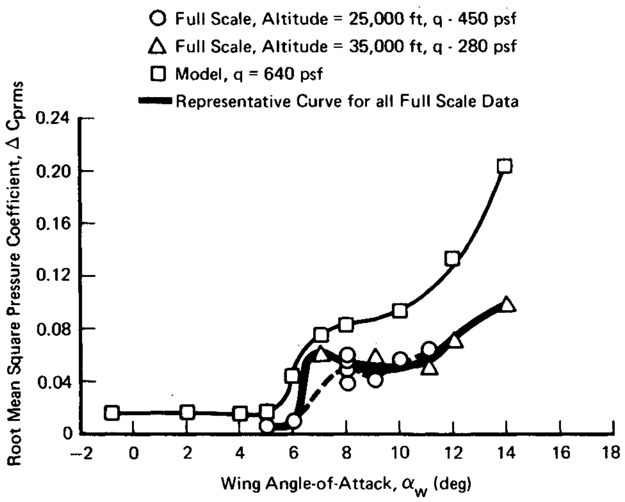

Fig. 8 Comparison of model and full scale rms pressure coefficient variation with angle-of-attack at Mach 0.9, 90% chord, 86% semispan.

Conclusions

Model data obtained from wind tunnel tests of a 10% scale YF-4E airplane have been analyzed and compared with full scale results. Random signal analysis was performed on fluctuating pressure transducer outputs which were then studied for spatial and spectral effects and for Mach number and angle-of-attack variation.

Validation of wind-tunnel pressure measurements made on the model was accomplished by comparison with flight data. Although limited by the small number of flight transducers, these comparisons showed good agreement in the spectral shapes. In general, the model rms levels were somewhat higher. Aircraft response predictions are therefore expected to be somewhat conservative.

Several pertinent conclusions drawn from the test data include the following:

At high angles-of-attack the flow pattern over a highly swept wing with a leading edge snag is quite complex. The flow close to the upper surface is strongly affected by

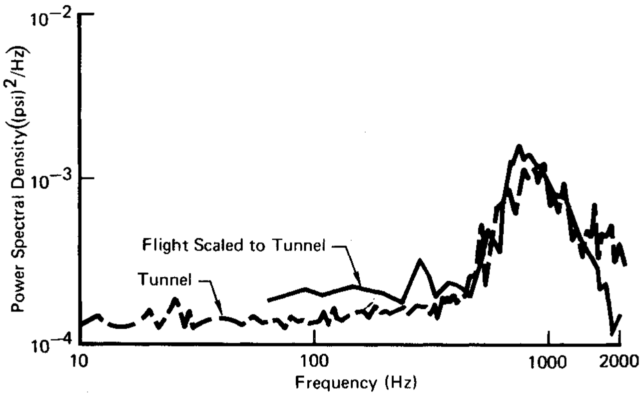

Fig. 10 Comparison of model and full scale pressure spectral shape (Mach 0.85, wing angle-of-attack 10°, transducer 18).

a vortex system consisting of leading edge, tip, and snag vortices causing abrupt changes in flow direction over the surface. The regions of high fluctuating pressures seem to be associated with these vortices, particularly the snag and tip vortices.

No discernible single "convection" mechanism for the transport of the fluctuating pressures was evident such as the downstream convection reported in studies of slender spacecraft launch vehicles. Disturbances seemed to emanate from multiple sources simultaneously and propagated in a complex manner.

Correlation is small between points on the wing that are separated by more than about ¼ of the mean aerodynamic chord.

The fluctuating pressure spectra frequently exhibited peaks at frequencies believed to be associated with vortices. The frequency associated with the snag vortex was generally about half that of the leading edge and tip vortices. These frequencies, scaled to the flight vehicle, were at the higher end of the vehicle's primary structural resonances.

Maximum buffet intensities occurred at the high subsonic Mach numbers diminishing abruptly to small values at sonic and supersonic speeds.

Maximum rms wing root bending moments caused by buffet were of the order of 7% of the corresponding steady bending moments.

Maximum fluctuating pressure coefficients were generally of the order of $\Delta C_{p_{rms}} = 0.2$.

The measurements from this model were used to establish a buffet spectral response method for computing wing vibrations; encouraging agreement with flight measurement was obtained.

References

[1]Cohen, M., "Buffet Characteristics of the Model F-4 Airplane in the Transonic Flight Regime," Air Force Rept. AFFDL-TR-70-56, April 1970, Air Force Flight Dynamics Lab., Wright-Patterson Air Force Base, Ohio.

[2]Titiriga, A., Jr., "F-5A Transonic Buffet Flight Test," Air Force Rept. AFFDL-TR-69-110, Dec. 1969, Air Force Flight Dynamics Lab., Wright-Patterson Air Force Base, Ohio.

[3]Cahill, J. F. and Stanewsky, E., "Wind Tunnel Tests of a Large-Chord, Swept-Panel Model to Investigate Shock-Induced Separation Phenomena," Air Force Rept. AFFDL-TR-69-78, Oct. 1969, Air Force Flight Dynamics Lab., Wright-Patterson Air Force Base, Ohio.

[4]Bies, D. A., "A Review of Flight and Wind Tunnel Measurements of Boundary Layer Pressure Fluctuations and Induced Structural Response," CR-626, Oct. 1966, NASA.

[5]Black, T. J., "An Analytical Study of the Measured Wall Pressure Field Under Supersonic Turbulent Boundary Layers," CR-888, April 1968, NASA.

[6]Hanson, P. W., "Evaluation of an Aeroelastic Model Technique for Predicting Airplane Buffet Loads," TN D-7066, Feb. 1973, NASA.

[7]Rose, R. and Nicholas, O. P., "Flight and Tunnel Measurements of Pressure Fluctuations on the Upper Surface of the Wing of a Venom Aircraft with a Sharpened Leading Edge," C.P. 1032, 1969, Aeronautical Research Council, England.

[8]Rainey, A. G., "Progress on the Launch-Vehicle Buffeting Problem," *Journal of Spacecraft and Rockets*, Vol. 2, No. 3, May–June 1965, pp. 289–299.

[9]Houbolt, J. C., "Structural Response of Reentry Vehicles to Boundary Layer Noise," ARAP Rept. 65, March 1965, Aeronautical Research Associates of Princeton, Princeton, N.J.

[10]Mullans, R. E. and Lemley, C. E., "Buffet Dynamic Loads During Transonic Maneuvers," Air Force Rept. AFFDL-TR-72-46, Sept. 1972, Air Force Flight Dynamics Lab., Wright-Patterson Air Force Base, Ohio.

MARCH 1974 J. AIRCRAFT VOL. 11, NO. 3

Some Aspects of Airfoil Stall in Low-Speed Flow

Hsiao C. Kao*
Northrop Corporation, Hawthorne, Calif.

In the process of reviewing some existing data on low-speed airfoil stalling, we find that it is possible to correlate the pressure distributions in the long bubbles of thin-airfoil stalling by using the reduced coordinates originally intended for the separation of base flow. The correlation so obtained bears close resemblance to the one for base flow. An existing correlation curve of leading-edge reseparation is used with measurements on a NACA 0010 and a NACA 66₃-018 airfoils to indicate the possibility of predicting the allowable angle of attack for maximum lift of moderately thick airfoils.

I. Introduction

THE stall of an airfoil is a very complex problem in aerodynamics. The mechanism itself is not fully understood and the parameters involved are many. Thus, it has so far defied theoretical treatment. Recourse is, therefore, made to experimental observations and measurements. Although some systematic efforts have been made, from which a few correlation curves resulted among other things, a large portion of the experimental results can only be found in the form of raw data. In view of this shortcoming, some existing data were re-examined from which we were able, a) to reduce the pressure distributions in the long bubble (thin-airfoil separation) to an almost single correlation curve, and b) to discover a possible utility of one existing correlation representation for predicting the maximum lift and occurrence of stall of a moderately thick airfoil.

Prior to any further discussion, it is worth stating the types of airfoil stall, since its demarcation is by no means unique. The common practice is to classify it into three major categories in low subsonic speed: a) the thin-airfoil stall, b) the leading-edge stall, and c) the trailing-edge stall.[1] The last type occurs generally on thick airfoils and it will not be considered here.

The thin-airfoil separation is usually observed on thin airfoils or on sharp leading-edge airfoils. The flow sepa-

Received August 8, 1973; revision received December 18, 1973. The author gratefully acknowledges the assistance of M. W. George and G. A. Feenstra for computation and drawing.

Index categories: Subsonic and Transonic Flow; Aircraft Performance.

*Senior Scientist, Aerodynamics Research.